

Ferromagnetism and giant magnetoresistance in the rare earth fullerides $\text{Eu}_{6-x}\text{Sr}_x\text{C}_{60}$

Kenji Ishii*

*Department of Physics, School of Science, The University of Tokyo,
7-3-1 Hongo, Bunkyo-ku, Tokyo 113-0033, Japan and
Synchrotron Radiation Research Center, Kansai Research Establishment,
Japan Atomic Energy Research Institute, 1-1-1 Kouto Mikazuki-cho Sayo-gun, Hyogo 679-5148, Japan*

Akihiko Fujiwara[†] and Hiroyoshi Suematsu[‡]

*Department of Physics, School of Science, The University of Tokyo,
7-3-1 Hongo, Bunkyo-ku, Tokyo 113-0033, Japan*

Yoshihiro Kubozono

*Department of Chemistry, Faculty of Science, Okayama University,
3-1-1 Tsushima-naka, Okayama 700-8530, Japan*

(Dated: February 2, 2022)

We have studied crystal structure, magnetism and electric transport properties of a europium fulleride Eu_6C_{60} and its Sr-substituted compounds, $\text{Eu}_{6-x}\text{Sr}_x\text{C}_{60}$. They have a *bcc* structure, which is an isostructure of other $M_6\text{C}_{60}$ (M represents an alkali atom or an alkaline earth atom). Magnetic measurements revealed that magnetic moment is ascribed to the divalent europium atom with $S = 7/2$ spin, and a ferromagnetic transition was observed at $T_C = 10 - 14$ K. In Eu_6C_{60} , we also confirm the ferromagnetic transition by heat capacity measurement. The striking feature in $\text{Eu}_{6-x}\text{Sr}_x\text{C}_{60}$ is very large negative magnetoresistance at low temperature; the resistivity ratio $\rho(H = 9 \text{ T})/\rho(H = 0 \text{ T})$ reaches almost 10^{-3} at 1 K in Eu_6C_{60} . Such large magnetoresistance is the manifestation of a strong π - f interaction between conduction carriers on C_{60} and $4f$ electrons of Eu.

PACS numbers: 61.48.+c, 75.50.-y, 72.80.Rj, 61.10.-i

I. INTRODUCTION

Since the discovery of fullerenes, C_{60} compounds have given us various opportunities for the research in condensed matter physics and materials science. Much attention was attracted to the superconductivity in A_3C_{60} (A is an alkali atom)¹. As for the magnetism, TDAE- C_{60} (TDAE is tetrakisdimethylaminoethylene) shows a ferromagnetic transition², while antiferromagnetic (or spin density wave) ground state was observed in polymeric A_1C_{60} ³, $\text{Na}_2\text{Rb}_{0.3}\text{Cs}_{0.7}\text{C}_{60}$ ⁴, and three-dimensional $(\text{NH}_3)\text{A}_3\text{C}_{60}$ ⁵. In these compounds a magnetic moment is considered to be carried by an electron on C_{60} molecule. Because various atoms and molecules can be intercalated into C_{60} crystal, we also expect the magnetic C_{60} compounds in which magnetic moment is carried by intercalants. In this viewpoint, rare earth metal is a good candidate. The research of rare earth fullerides was reported for Yb ⁶ and Sm ⁷ in relation to the superconductivity, but little effort has been made to study the magnetic properties. The only case of magnetic study in rare earth fullerides is for europium. Europium has a magnetic moment of $7\mu_B$ ($S = 7/2$, $L = 0$, and $J = 7/2$) in the divalent state, while it is non-magnetic ($S = 3$, $L = 3$, and $J = 0$) in the trivalent state. A photoemission study of C_{60} overlaid on Eu metal revealed the charge transfer from Eu to C_{60} and the formation of fulleride⁸. Ksari-Habiles *et al.*^{9,10} investigated the crystal structure and magnetic properties of $\text{Eu}_{\sim 3}\text{C}_{60}$ and Eu_6C_{60} ; they observed some magnetic anomalies in Eu_6C_{60} .

In this paper, we report the ferromagnetic transition of Eu_6C_{60} , which was observed at $T_C \sim 12$ K in magnetic and heat capacity measurements. We also investigated the substitution effect from Eu to non-magnetic Sr, and the ferromagnetic transition temperature was found to change little with the Sr concentration. In the resistivity measurement we found a huge negative magnetoresistance below around T_C ; the reduction ratio of resistivity $\rho(H)/\rho(0)$ is almost 10^{-3} at 1 K in Eu_6C_{60} . This ratio is comparable to those in perovskite manganese oxides, which is known as colossal magnetoresistance (CMR). However Eu_6C_{60} should be categorized as a new class of giant magnetoresistive compounds in the sense that (1) the magnitude of magnetoresistance increases very steeply with decreasing temperature rather than the vicinity of T_C , (2) the compound consists of a molecule with novel structure. These features can open the further possibility to find a new magnetic and magnetoresistive material.

II. EXPERIMENTAL PROCEDURES

Polycrystalline samples of $\text{Eu}_{6-x}\text{Sr}_x\text{C}_{60}$ were synthesized by solid-state reaction. A stoichiometric amount of mixture of Eu, Sr and C_{60} powders, which was pressed into a pellet and sealed in a quartz tube in vacuum, was heat-treated at 600 °C for about 10 days. In the course of the heat treatment the sample was ground for ensuring the complete reaction. Because the sample is very

unstable in air, we treated it in a glove box with inert atmosphere.

Powder x-ray diffraction experiments were carried out by using synchrotron radiation x-rays at BL-1B in Photon Factory, KEK, Tsukuba. The samples were put into a glass capillary in 0.3 mm diameter and an imaging plate was used for the detection¹¹. Magnetic measurements were performed using a SQUID magnetometer. In the heat capacity measurement by relaxation method, the sample was pressed into a pellet and sealed by grease to keep from exposure to air. Eu L_{III} -edge XANES (x-ray absorption near edge structure) was measured in the fluorescence method at BL01B1 of SPring-8, Harima. The resistivity measurements were carried out by the 4-probe method. Four gold wires were attached to a pressed pellet of polycrystalline sample with sliver paste. The sample was put into a capsule and sealed in He atmosphere.

III. RESULTS

X-ray diffraction spectra of $\text{Eu}_{6-x}\text{Sr}_x\text{C}_{60}$ are shown in Fig. 1(a). The spectrum of Sr_6C_{60} is also presented as a reference. The wavelength of x-ray is 0.8057 Å for $x = 0, 3, 5$, and 0.8011 Å for $x = 6$. They all can be understood by a *bcc* structure which is an isostructure of other $M_6\text{C}_{60}$ in alkali¹², alkaline earth¹³ and rare earth (Sm)¹⁴ fullerenes. The Rietveld refinements based on the space group $Im\bar{3}$ were performed with use of the RIETAN program^{15,16}. In the refinements, only two atomic coordinates (x for C1 and C3) are refined in C_{60} molecule, which corresponds to the refinement of the length of 6:6 bond (the bond between two hexagons) and 5:6 bond (the bond between hexagon and pentagon). In the compounds of $x = 3$ and 5, the sum of the metal concentration is fixed to unity. The results of refinement are presented in Table I and obtained structure is shown in Fig. 1(b). This crystal structure of Eu_6C_{60} is consistent with the previous works^{10,17}, but we observed little trace of the secondary phase in the present sample. In the Sr-substituted compounds, the values of Eu concentration are in good agreement with the nominal ones.

As seen in Fig. 1(c), the obtained lattice constants change linearly with the nominal Eu concentration, which means they follow the Vegard's law, and confirms the formation of solid solution at $x = 3$ and 5. This result is attributed to the fact that ionic radius of Eu^{2+} and Sr^{2+} is quite similar, while the substitution of Ba for Eu results in the phase separation.

Figures 2 show the result of magnetic measurements of $\text{Eu}_{6-x}\text{Sr}_x\text{C}_{60}$. Above 30 K, magnetic susceptibility (χ) follows the Curie-Weiss law, as shown in Figs. 2(a)-(c). The effective Bohr magneton estimated from Curie constant and the Weiss temperature are summarized in Table II¹⁸. The former agrees with the Eu^{2+} state ($S = 7/2$, $L = 0$, and $J = 0$). The field dependence of magnetization at 2 K gives the saturation moment close to $7\mu_B$, which is consistent with the magnetic moment of

Eu^{2+} . Moreover the Eu^{2+} state has been also confirmed by Eu L_{III} -edge XANES experiments, as seen in Fig. 3. The spectra of EuS and Eu_2O_3 was also presented as a reference of divalent and trivalent of Eu, and absorption edges of $\text{Eu}_{6-x}\text{Sr}_x\text{C}_{60}$ are very close to that of EuS. The divalent state of Eu also observed in the case that Eu atom exists inside the C_{60} cage, namely, metallofullerene $\text{Eu}@\text{C}_{60}$ ¹⁹.

Temperature dependence of magnetization at a weak field of 3 mT (Figs. 2(g)-(i)) shows a steep increase of magnetization below 10-14 K, indicating a ferromagnetic transition. To confirm the presence of the ferromagnetic phase transition, we measured heat capacity for Eu_6C_{60} . In Fig. 2(g) we show the temperature dependence of heat capacity including that of grease. An obvious peak can be seen near the transition temperature, which is an evidence of the ferromagnetic phase transition. The T_C is determined to be 11.6 K from the peak position. We ascertained that there was no anomaly in specific heat in this temperature region for grease, which was used to keep the sample from exposure to air. We can also see a smaller peak near 16 K, whose origin has not been clarified yet, but we consider that it does not come from a magnetic origin because of no anomaly in the temperature dependence of magnetization. The transition temperatures for $\text{Eu}_3\text{Sr}_3\text{C}_{60}$ and $\text{Eu}_1\text{Sr}_5\text{C}_{60}$ are estimated from the Arrott plot²⁰ at 12.8 K and 10.4 K, respectively. These values are very close to the Weiss temperature mentioned above. In Eu_6C_{60} , the transition temperature estimated from the Arrott plot is a little larger value (13.7 K) than that from the heat capacity measurement, but it is not so important in the following discussion.

From these evidences we conclude that $\text{Eu}_{6-x}\text{Sr}_x\text{C}_{60}$ shows a ferromagnetic transition at $T_C = 10\text{-}14$ K, and the magnetic moment is ascribed to Eu^{2+} . In the previous work of Eu_6C_{60} , Ksari-Habiles *et al.*⁹ observed a mixed valence state of Eu (Eu^{2+} and Eu^{3+}) and three successive magnetic anomalies, which is different from the present work; a possible reason is that their sample might contain a secondary phase other than Eu_6C_{60} .

Figure 4 (a) shows the temperature dependence of electric resistivity of Eu_6C_{60} measured at some magnetic fields. A most striking feature in resistivity is the huge negative magnetoresistance below around T_C . The negative magnetoresistance becomes much more significant at lower temperature. In the case of Eu_6C_{60} , magnetoresistivity $\rho(H = 9 \text{ T})$ is three orders magnitude smaller than $\rho(H = 0 \text{ T})$ at 1 K, as seen in Fig. 4 (b). This large negative magnetoresistance is comparable to those of the colossal magnetoresistance (CMR) materials such as perovskite manganese oxides, where CMR effect is seen only near the ferromagnetic transition temperature. We also observed a relatively large magnetoresistance in the Sr-substituted compounds, as shown in 4 (c). There is no difference between magnetoresistances in the transverse ($H \perp I$) and longitudinal ($H \parallel I$) configurations (I represents electric current), suggesting the magnetoresistance

in Eu_6C_{60} is not ascribed to the orbital motion of free carriers.

IV. DISCUSSION

Such giant magnetoresistance is a manifestation of the strong interaction between conduction carriers and localized magnetic moments; namely, the strong π - f interaction exists in Eu_6C_{60} . When we consider formal valence state of $(\text{Eu}^{2+})_6\text{C}_{60}^{12-}$, t_{1g} band of C_{60} is completely filled and the compound should become an insulator. In this case, the interaction between conduction carrier and localized moment is considered to be weak, assuming that the conduction carrier mainly passes on C_{60} molecules. If Eu orbitals hybridize with C_{60} orbitals and form a part of conduction band, much enhancement of the interaction must occur. In the band calculation for Sr_6C_{60} and Ba_6C_{60} ²¹ which have the same *bcc* crystal structure and the same valence state as Eu_6C_{60} , the hybridization of the d orbital of metal atom and the t_{1g} orbital of C_{60} exists and make the compounds metallic. This fact is confirmed experimentally²². The hybridization is more significant in Sr_6C_{60} than Ba_6C_{60} due to the smaller lattice constant of Sr_6C_{60} . The band structure of Eu_6C_{60} has not been studied yet, but such hybridization of the $5d$ and/or $6s$ orbitals of Eu and the t_{1g} orbital of C_{60} is plausible in Eu_6C_{60} because Eu_6C_{60} has a further smaller lattice constant than Sr_6C_{60} .

The π - f interaction is likely to affect to magnetic interaction of $4f$ electrons and the origin of ferromagnetism in Eu_6C_{60} may be ascribed to the indirect exchange interaction. In the *bcc* structure, an Eu atom has 4 nearest neighbor Eu atoms (the distance between two Eu atoms is 3.89 Å). Therefore, in the case of $\text{Eu}_1\text{Sr}_5\text{C}_{60}$, 5 of 6 Eu atoms are replaced by non-magnetic Sr atoms, Eu atoms can no longer have the three-dimensional Eu network, so that the direct interaction fails completely. Nevertheless T_C does not show a drastic change. This is a quite contrast with the case of magnetic semiconductor EuO, where the direct exchange interaction between Eu atoms is important²³ and the substitution of Ca for Eu significantly reduces the ferromagnetic transition temperature²⁴. This fact indicates that the ferromagnetism in Eu_6C_{60} comes from the indirect exchange interaction via C_{60} molecules, and the π - f interaction has an important role in the present system.

Now we discuss the origin of the giant magnetoresistance. The features of magnetoresistance in Eu_6C_{60} are (1) negative magnetoresistance occurs below around T_C , (2) saturation field of magnetization is close to that of magnetoresistance ratio ($\rho(H)/\rho(0)$), as seen in the top curve of Fig. 2(d) and the bottom curve of Fig. 4(c), (3) magnetoresistance is much enhanced at lower temperatures; The magnetoresistance ratio ($\rho(H)/\rho(0)$) does not seem to saturate with decreasing temperature, while the magnetization almost saturates at 2 K and 5.5 T. The feature (1) indicates that the present MR is closely

related to the ferromagnetic transition. In usual ferromagnetic metal, spin fluctuation scatters conduction electrons and causes negative magnetoresistance^{25,26}. This effect may be an origin of the magnetoresistance near T_C , but this is not the case for the giant magnetoresistance in Eu_6C_{60} at lower temperature, because such effect is remarkable in the vicinity of T_C inconsistent with the feature (3). The feature (2) suggests that magnetoresistance is related to the magnetization. Furthermore, when we see $\rho(H)/\rho(0)$ in log scale, the difference of $\rho(H)/\rho(0)$ between 2 K and 1 K is almost one order (Fig. 4(b)), while that of magnetization must be small. This means there is another factor, in addition to the magnetization, to determine the magnetoresistance. It is probably temperature, that is, an activation process needs to be considered in the origin of the magnetoresistance.

One possible interpretation of magnetoresistance in Eu_6C_{60} is the spin-dependent tunneling at the grain boundary²⁷. In the case of ferromagnetic granular metal, the conductivity is dependent on the tunneling probability of carriers through insulating barrier between grains, and the probability crucially depends on the spin polarization of carriers. In this case, each grain is assumed to be conductive and surrounded by less conductive surface. Because we measured the resistivity in a pellet of polycrystalline sample and Eu_6C_{60} is very unstable in air, the surface may react to be insulative barrier, even if the sample is treated in high purity inert atmosphere. However we should note that the insulating region is considered to be limited only on the thin surface because unidentified peaks in XRD spectrum are very weak and they are considered not to affect to the magnetic and heat capacity measurements. As shown in the inset of Fig. 4(a), the temperature dependence of resistivity is represented as $\rho(T) \propto \exp(T_0/T)^{1/\alpha}$ ($\alpha \sim 2$), rather than the activation type which is expected in a usual semiconductor. The value of T_0 is about 180 K at 0T. This fact suggests that the resistivity in our sample might be governed by the tunneling at the boundaries²⁸. Our preliminary Hall effect measurement gives $R_H = +5 \times 10^{-2} \text{ cm}^3/\text{C}$ at 250 K, corresponding to the hole density of $1 \times 10^{20} \text{ cm}^{-3}$ (0.1 hole per C_{60}); this means that intrinsic Eu_6C_{60} can have relatively high conductivity and is possibly metallic by hybridization of the C_{60} and metal orbitals mentioned above. Note that Hall voltage is less sensitive to the grain boundary effect. Helman and Abeles²⁷ considered the magnetic exchange energy E_M and gave the magnetoconductivity as

$$\sigma(H, T) = \sigma_0 [\cosh(E_M/2k_B T) - P \sinh(E_M/2k_B T)], \quad (1)$$

where P is the spin polarization of carrier and $E_M = (1/2)J[1-m^2]$. J is the exchange coupling constant between a conduction carrier and a ferromagnetic metal grain and m is the magnetization normalized by the saturation value. The equation (1) gives a negative magnetoresistance of orders of magnitude only when P is very

close to unity. If $P = 1$, we obtain

$$\rho(H)/\rho(0) = \exp(-Jm^2/4k_B T). \quad (2)$$

Magnetoresistance in equation (2) becomes large with decreasing temperature, which agree qualitatively with the feature (2) mentioned above. The assumption of $P = 1$ might be unrealistic in usual ferromagnetic metals. However, if the exchange interaction between Eu atoms is accomplished via π -bands of C_{60} as discussed earlier, we can expect a large spin polarization of π -electrons.

We can also consider the effect of magnetic polaron. In magnetic semiconductors such as Eu chalcogenides, a carrier makes surrounding magnetic moments be polarized via exchange interaction and forms a magnetic polaron²⁹. At zero field, magnetic polarons have to move with flipping some magnetic moments which are more or less randomly oriented, and their conduction is suppressed. Application of magnetic field aligns spin directions and carriers become mobile. As a result, negative magnetoresistance occurs. The negative magnetoresistance above T_C can be attributed to this picture. Even in the ferromagnetic phase, magnetic moments have to be flipped at a magnetic domain boundary for the motion of carrier. Because remnant magnetic moment is little, as seen in Figs. 2 (d), many magnetic domains exist in our sample of Eu_6C_{60} . The crucial point of above two interpretations (spin dependent tunneling and magnetic polaron) are that carriers must overcome large exchange interaction with localized spins when they go into the region of different orientation of magnetic moments.

V. SUMMARY

We have measured crystal structure, magnetic properties and magnetoresistance in polycrystalline Eu_6C_{60} and its Sr-substituted compounds, $Eu_{6-x}Sr_xC_{60}$. They all have a *bcc* structure and the compounds of $x = 3$ and 5 form a solid solution concerning the occupation of metal atom. A ferromagnetic transition is observed at $T_C \sim 12$ K in Eu_6C_{60} and all Eu atoms are in divalent state with a magnetic moment of $7\mu_B$ ($S = 7/2$). The fact that the substitution of non-magnetic Sr for Eu affects little to T_C indicates the ferromagnetic interaction is caused through the conduction carriers. In the resistivity measurement, we have found that Eu_6C_{60} showed a huge negative magnetoresistance and $\rho(H)/\rho(0)$ reduced almost 10^{-3} at $H = 9$ T and $T = 1$ K. The precise mechanism of magnetoresistance has not clarified yet, but it manifests a strong interaction between π -conduction electrons of C_{60} and $4f$ electrons on Eu.

Acknowledgments

We acknowledge to Prof. Y. Iwasa, Dr. T. Takenobu and S. Moriyama for the suggestions for synthesis and heat capacity measurements. We also thank to Prof. A. Asamitsu for the advice of the resistivity measurements at low temperature. This work was supported by “Research for the Future” of Japan Society for the Promotion of Science (JSPS), Japan.

* Electronic address: kenji@spring8.or.jp

† Present address: School of Materials Science, Japan Advanced Institute of Science and Technology, 1-1 Asahidai, Tatsunokuchi, Ishikawa 923-1292, Japan

‡ Present address: Material Science Division, SR Research Laboratory, Japan Synchrotron Radiation Research Institute, 1-1-1 Kouto Mikazuki-cho, Sayo-gun, Hyogo 679-5198, Japan

¹ A. F. Hebard, M. J. Rosseinsky, R. C. Haddon, D. W. Murphy, S. H. Glarum, T. T. M. Palstra, A. P. Ramirez, and A. R. Kortan, *Nature (London)* **350**, 600 (1991).

² P. M. Allemand, K. C. Khemani, A. Koch, F. Wudl, K. Holczer, S. Donovan, G. Grüner, and J. D. Thompson, *Science* **253**, 301 (1991).

³ O. Chauvet, G. Oszlányi, L. Forro, P. W. Stephens, M. Tegze, G. Faigel, and A. Jánossy, *Phys. Rev. Lett.* **72**, 2721 (1994).

⁴ D. Arčon, K. Prassides, A. L. Maniero, and L. C. Brunel, *Phys. Rev. Lett.* **84**, 562 (2000).

⁵ T. Takenobu, T. Muro, Y. Iwasa, and T. Mitani, *Phys. Rev. Lett.* **85**, 381 (2000).

⁶ E. Özdağ, A. R. Kortan, N. Kopylov, A. P. Ramirez, T. Siegrist, K. M. Rabe, H. E. Bair, S. Schuppler, and P. H. Citrin, *Nature (London)* **375**, 126 (1995).

⁷ X. H. Chen and G. Roth, *Phys. Rev. B* **52**, 15534 (1995).

⁸ H. Yoshikawa, S. Kuroshima, I. Hirokawa, K. Tanigaki, ,

and J. Mizuki, *Chem. Phys. Lett.* **239**, 103 (1995).

⁹ Y. Ksari-Habiles, D. Claves, G. Chouteau, P. Touzain, C. Jeandey, J. L. Oddoou, and A. Stepanov, *J. Phys. Chem. Solids* **58**, 1771 (1997).

¹⁰ D. Claves, Y. Ksari-Habiles, G. Chouteau, and P. Touzain, *Solid State Commun.* **106**, 431 (1998).

¹¹ A. Fujiwara, K. Ishii, T. Watanuki, H. Suematsu, H. Nakao, K. Ohwada, Y. Fujii, Y. Murakami, T. Mori, H. Kawada, et al., *J. Appl. Cryst.* **33**, 1241 (2000).

¹² O. Zhou, J. E. Fisher, N. Coustel, S. Kycia, Q. Zhu, A. R. McGhie, W. J. Romanow, J. P. M. Jr., A. B. S. III, and D. E. Cox, *Nature (London)* **351**, 462 (1991).

¹³ A. R. Kortan, N. Kopylov, S. Glarum, E. M. Gyorgy, A. P. Ramirez, R. M. Fleming, O. Zhou, F. A. Thiel, P. L. Trevor, and R. C. Haddon, *Nature (London)* **360**, 566 (1991).

¹⁴ X. H. Chen, Z. S. Liu, S. Y. Li, D. H. Chi, and Y. Iwasa, *Phys. Rev. B* **60**, 6183 (1999).

¹⁵ F. Izumi, in *The Rietveld Method*, edited by R. A. Young (Oxford University Press, Oxford, 1993), chap. 13.

¹⁶ Y. I. Kim and F. Izumi, *J. Ceram. Soc. Jpn.* **102**, 401 (1994).

¹⁷ H. Ootoshi, K. Ishii, A. Fujiwara, T. Watanuki, Y. Mat-suoka, and H. Suematsu, *Mol Cryst. and Liq. Cryst.* **340**, 565 (2000).

¹⁸ In $Eu_3Sr_3C_{60}$ and $Eu_1Sr_5C_{60}$, the values of μ_{eff} and M_S

in Tabel II are a little larger than the theoretical values of Eu^{2+} . The most probable reason is the discrepancy of the stoichiometry, but the excess from the theoretical value is often observed in the samples of different batches, including Eu_6C_{60} .

- ¹⁹ T. Inoue, Y. Kubozono, S. Kashino, Y. Takabayashi, K. Fujitaka, M. Hida, M. Inoue, T. Kambara, S. Emura, and T. Uruga, Chem. Phys. Lett. **316**, 381 (2000).
²⁰ A. Arrott, Phys. Rev. **108**, 1394 (1957).
²¹ S. Saito and A. Oshiyama, Phys. Rev. Lett. **71**, 121 (1993).
²² B. Gogia, K. Kordatos, H. Suematsu, K. Tanigaki, and K. Prassides, Phys. Rev. B **58**, 1077 (1998).
²³ T. Kasuya, I.B.M. J. Res. Develop. **14**, 214 (1970).
²⁴ A. A. Samokhvalov, N. N. Loshkareva, and V. G. Bamburov, Sov. Phys. Solid State **9**, 555 (1967).
²⁵ P. G. E. de Gennes and J. Friedel, J. of Phys. Chem. Solids **4**, 71 (1958).
²⁶ M. E. Fisher and J. S. Langer, Phys. Rev. Lett. **20**, 665 (1968).
²⁷ J. S. Helman and B. Abeles, Phys. Rev. Lett. **37**, 1429 (1976).
²⁸ P. Sheng, B. Abeles, and Y. Arie, Phys. Rev. Lett. **31**, 44 (1972).
²⁹ T. Kasuya and A. Yanase, Rev. Mod. Phys. **40**, 684 (1968).

TABLE I: Structural parameter obtained from the Rietveld refinement of $\text{Eu}_{6-x}\text{Sr}_x\text{C}_{60}$.

Eu_6C_{60} $a_0 = 10.940 \pm 0.001 \text{ \AA}$ $R_{wp} = 3.81 \%$						
Site	Occupancy	x	y	z	$B(\text{\AA}^2)$	
C1	24g	1	0.0672(5)	0	0.3200	0.5(2)
C2	48h	1	0.1325	0.1056	0.2797	0.5
C3	48h	1	0.0653(3)	0.2144	0.2381	0.5
Eu^{2+}	12e	1	0	0.5	0.2768(2)	2.29(4)
$\text{Eu}_3\text{Sr}_3\text{C}_{60}$ $a_0 = 10.958 \pm 0.002 \text{ \AA}$ $R_{wp} = 6.20 \%$						
Site	Occupancy	x	y	z	$B(\text{\AA}^2)$	
C1	24g	1	0.0686(6)	0	0.3186	1.1(3)
C2	48h	1	0.1328	0.1038	0.2790	1.1
C3	48h	1	0.0641(4)	0.2148	0.2366	1.1
Eu^{2+}	12e	0.51(2)	0	0.5	0.2792(3)	2.99(7)
Sr^{2+}	12e	0.49	0	0.5	0.2792	2.99
$\text{Eu}_1\text{Sr}_5\text{C}_{60}$ $a_0 = 10.971 \pm 0.002 \text{ \AA}$ $R_{wp} = 6.37 \%$						
Site	Occupancy	x	y	z	$B(\text{\AA}^2)$	
C1	24g	1	0.0660(5)	0	0.3207	2.1(3)
C2	48h	1	0.1321	0.1069	0.2798	2.1
C3	48h	1	0.0661(3)	0.2138	0.2390	2.1
Eu^{2+}	12e	0.18(2)	0	0.5	0.2803(3)	2.73(6)
Sr^{2+}	12e	0.82	0	0.5	0.2803(3)	2.73
Sr_6C_{60} $a_0 = 10.986 \pm 0.002 \text{ \AA}$						

TABLE II: Summary of the magnetic properties of $\text{Eu}_{6-x}\text{Sr}_x\text{C}_{60}$. μ_{eff} , Θ , M_S , and T_C denote effective Bohr magneton ($g_J\sqrt{J(J+1)}\mu_B$), Weiss temperature, saturation moment, and ferromagnetic transition temperature, respectively.

	$\mu_{eff}/\text{Eu} (\mu_B)$	$\Theta (\text{K})$	$M_S/\text{Eu} (\mu_B)$	$T_C (\text{K})$
Eu^{2+}	7.94		7	
Eu_6C_{60}	7.77	10.6	6.97	11.6 ^a (13.7 ^b)
$\text{Eu}_3\text{Sr}_3\text{C}_{60}$	8.13	12.6	7.73	12.8 ^b
$\text{Eu}_1\text{Sr}_5\text{C}_{60}$	8.26	8.0	7.68	10.4 ^b

^aFrom the peak position of heat capacity measurement.

^bFrom the Arrott plot.

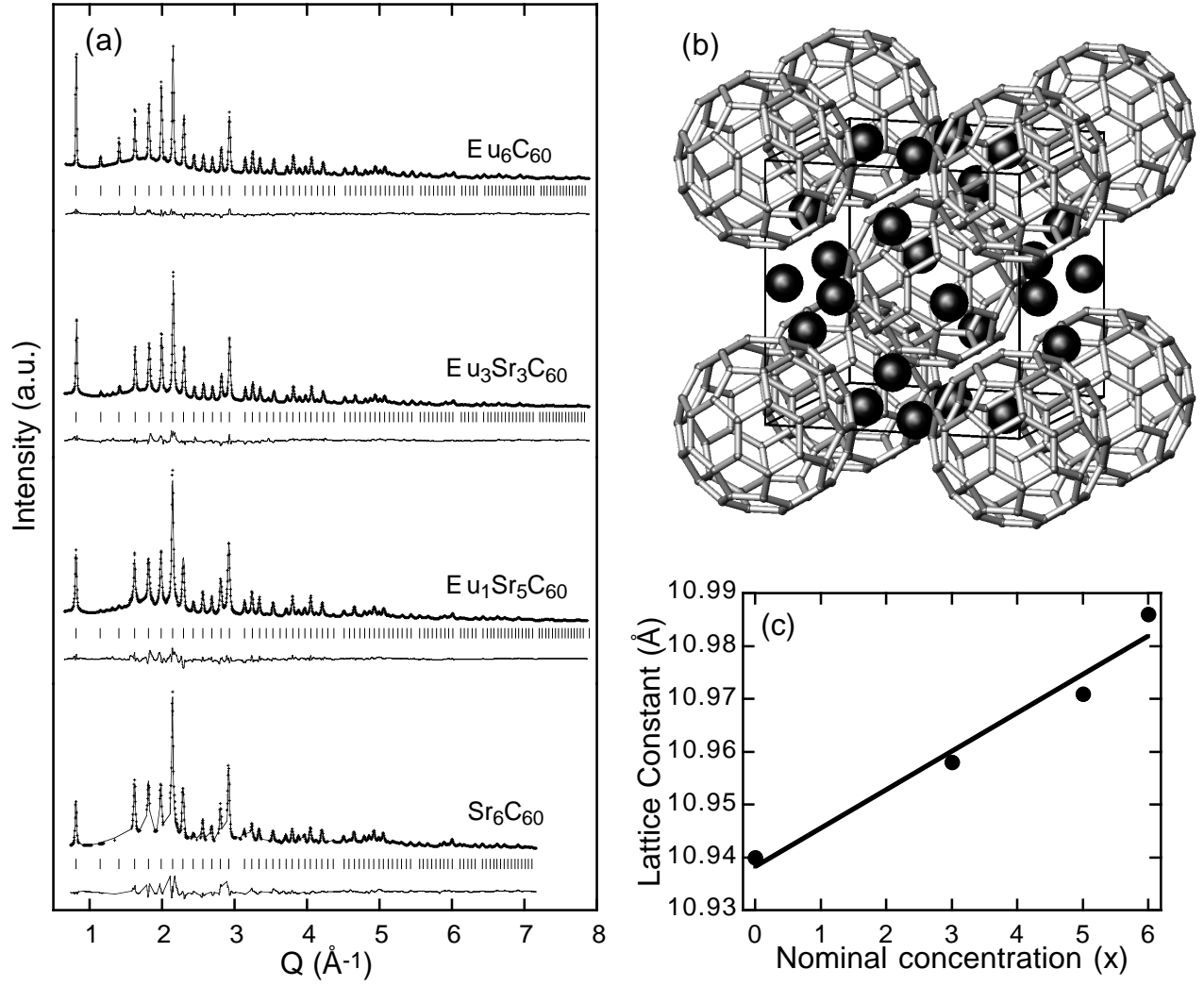


FIG. 1: (a) X-ray diffraction spectra of $\text{Eu}_{6-x}\text{Sr}_x\text{C}_{60}$. The wavelength of x-ray is 0.8057 \AA for $x = 0, 3, 5$, and 0.8011 \AA for $x = 6$. (b) Schematic view of the crystal structure of $\text{Eu}_{6-x}\text{Sr}_x\text{C}_{60}$. The black ball represents a metal atom. (c) Lattice constant vs. nominal concentration of Eu (x). The lattice constant changes linearly with x , following the Vegard's law.

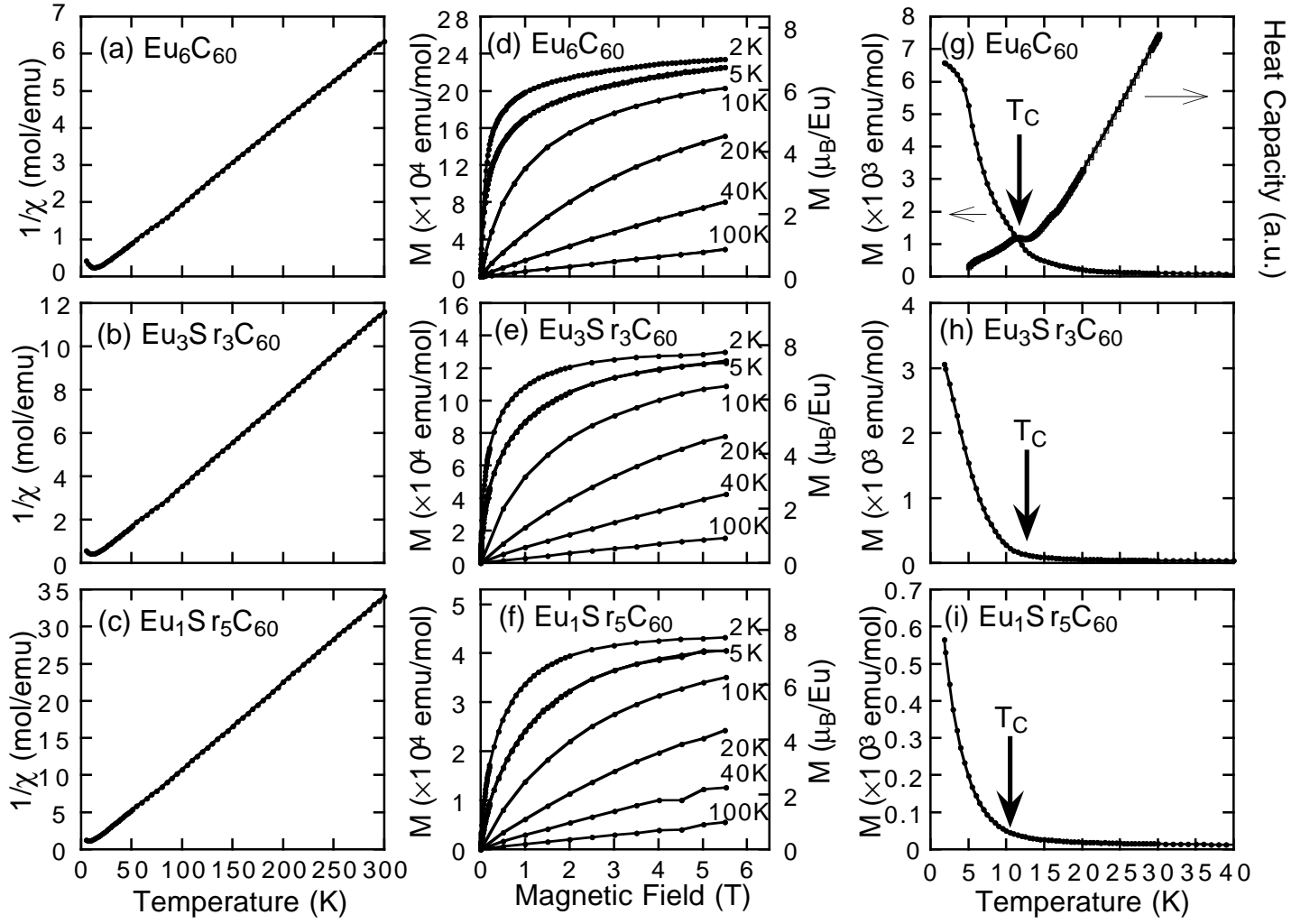


FIG. 2: (a)-(c) Inverse magnetic susceptibility obtained from the magnetization at 1 and 2 T. (d)-(f) Magnetization curve. (g)-(i) Temperature dependence of the magnetization at 3 mT. Heat Capacity of Eu_6C_{60} is also presented in (g). The arrows indicate the ferromagnetic transition temperatures determined the peak position of the heat capacity measurement for Eu_6C_{60} , and estimated from the Arrott plot for $\text{Eu}_3\text{Sr}_3\text{C}_{60}$ and $\text{Eu}_1\text{Sr}_5\text{C}_{60}$.

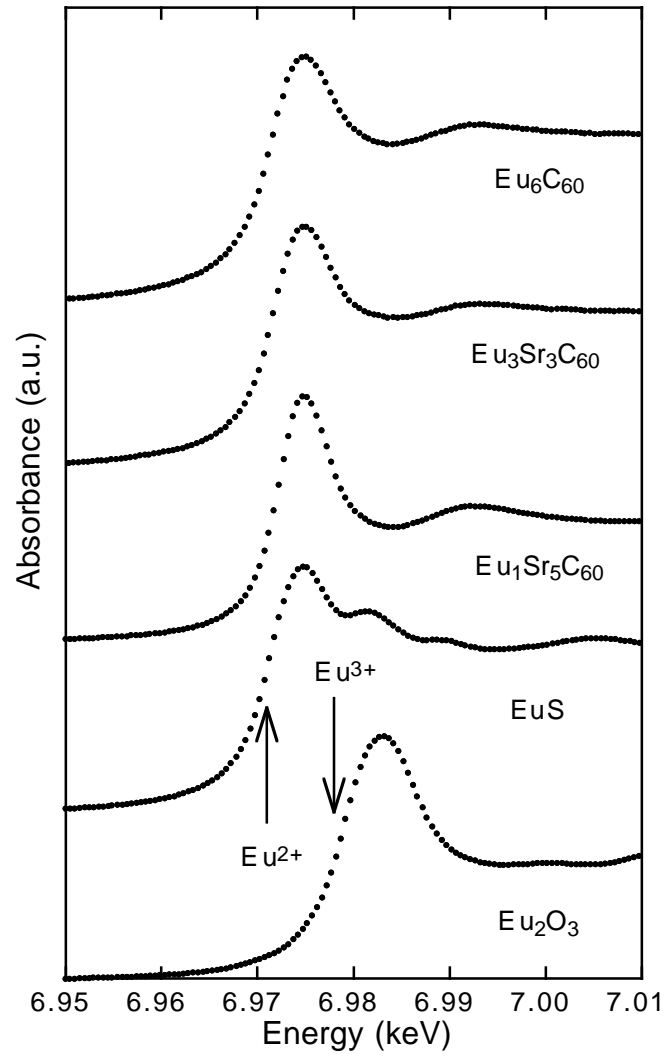


FIG. 3: XANES spectra of $\text{Eu}_{6-x}\text{Sr}_x\text{C}_{60}$. The arrows indicate the absorption edge in divalent and trivalent reference.

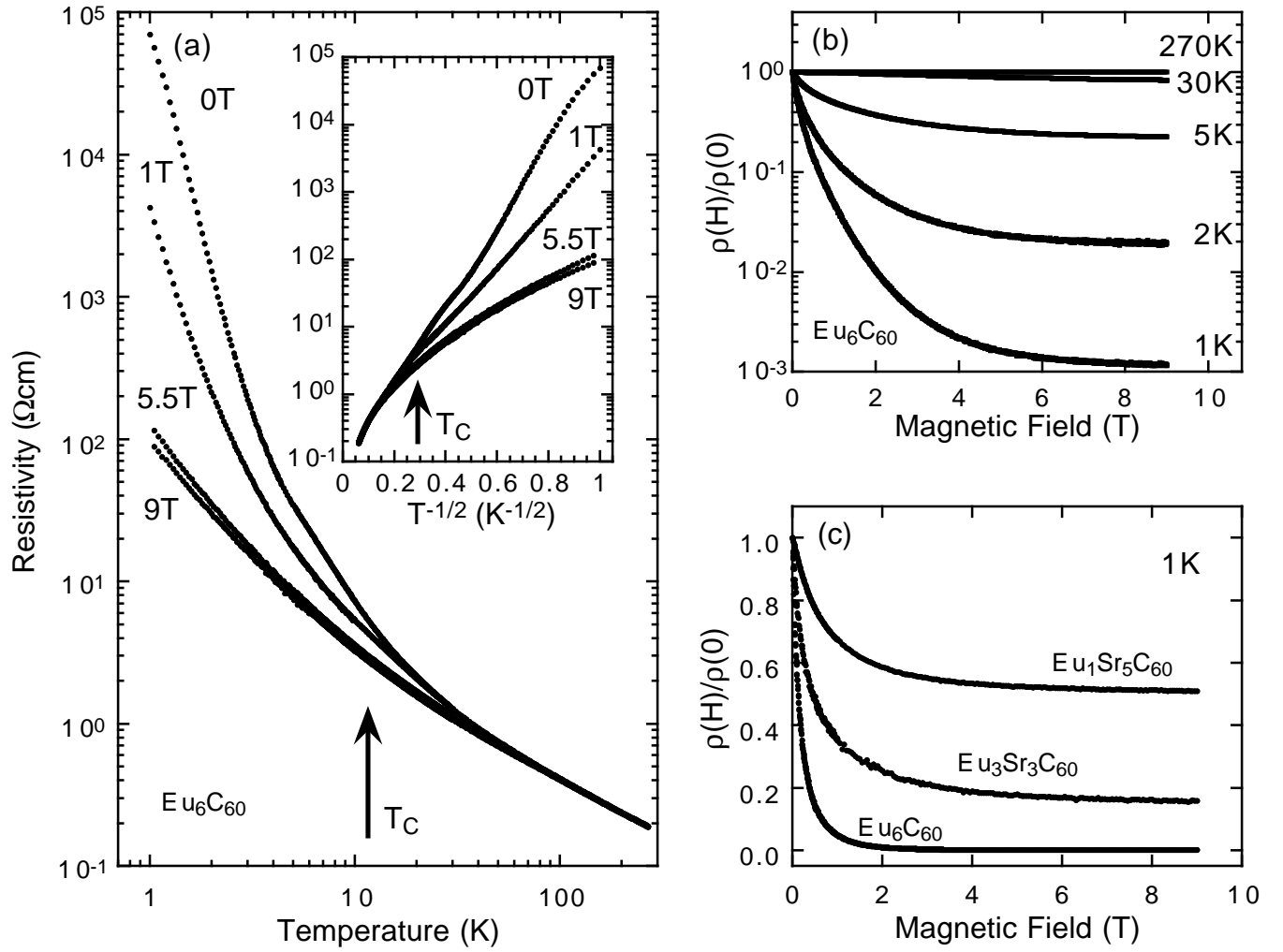


FIG. 4: (a) Temperature dependence of resistivity of polycrystalline Eu_6C_{60} at some magnetic fields. The arrow indicates the ferromagnetic transition temperature. (b) Magnetic field dependence of resistivity of Eu_6C_{60} normalized at zero field for some temperatures. (c) Magnetic field dependence of resistivity of $\text{Eu}_{6-x}\text{Sr}_x\text{C}_{60}$ normalized at zero field measured at 1 K.